On Battery Recovery Effect in Wireless Sensor Nodes

Swaminathan Narayanaswamy, TUM CREATE Limited
Steffen Schlueter, TUM CREATE Limited
Sebastian Steinhorst, TUM CREATE Limited
Martin Lukasiewycz, TUM CREATE Limited
Samarjit Chakraborty, Technical University of Munich
Harry Ernst Hoster, Lancaster University

With the perennial demand for longer runtime of battery-powered Wireless Sensor Nodes (WSNs), several techniques have been proposed to increase the battery runtime. One such class of techniques exploiting the *battery recovery effect* phenomenon claims that performing an intermittent discharge instead of a continuous discharge will increase the usable battery capacity. Several works in the areas of embedded systems and wireless sensor networks have assumed the existence of this recovery effect and proposed different power management techniques in the form of power supply architectures (multiple battery setup) and communication protocols (burst mode transmission) in order to exploit it. However, until now, a systematic experimental evaluation of the recovery effect has not been performed with real battery cells, using high accuracy battery testers to confirm the existence of this recovery phenomenon. In this paper, a systematic evaluation procedure is developed to verify the existence of this battery recovery effect. Using our evaluation procedure we investigated Alkaline, Nickel-Metal Hydride (NiMH) and Lithium-Ion (Li-Ion) battery chemistries, which are commonly used as power supplies for WSN applications. Our experimental results do not show any evidence of the aforementioned recovery effect in these battery chemistries. In particular, our results show a significant deviation from the stochastic battery models, which were used by many power management techniques. Therefore, the existing power management approaches that rely on this recovery effect do not hold in practice. Instead of a battery recovery effect, our experimental results show the existence of the *rate capacity effect*, which is the reduction of usable battery capacity with higher discharge power, to be the dominant electrochemical phenomenon that should be considered for maximizing the runtime of WSN applications. We outline power management techniques that minimize the rate capacity effect in order to obtain a higher energy output from the battery.

CCS Concepts: •**General and reference** → **Experimentation;** •**Networks** → **Sensor networks;** •**Hardware** → **Batteries; Wireless devices;**

General Terms: Design, Performance, Experimentation, Measurement

Additional Key Words and Phrases: Batteries, wireless sensor nodes, recovery effect, battery modeling, power management, battery operated electronics.

ACM Reference Format:
Swaminathan Narayanaswamy, Steffen Schlueter, Sebastian Steinhorst, Martin Lukasiewycz, Samarjit Chakraborty, and Harry Ernst Hoster, 2016. On Battery Recovery Effect in Wireless Sensor Nodes. *ACM Trans. Des. Autom. Electron. Syst.* 00, 00, Article 00 (2016), 28 pages.
DOI: http://dx.doi.org/10.1145/0000000.0000000

This work was financially supported by the Singapore National Research Foundation under its Campus for Research Excellence and Technological Enterprise (CREATE) programme.
Author's addresses: S. Narayanaswamy (corresponding author) and S. Steinhorst and M. Lukasiewycz, Embedded Systems Department, TUM CREATE Limited, Singapore; corresponding author's email:swaminathan.narayana@tum-create.edu.sg. S. Schlueter, Department of Electrochemistry and New Materials, TUM CREATE Limited, Singapore; S. Chakraborty, Institute for Real-time Computer Systems, Technical University of Munich, Germany; H. E. Hoster, Chemistry Department, Lancaster University, United Kingdom.

DOI: http://dx.doi.org/10.1145/0000000.0000000

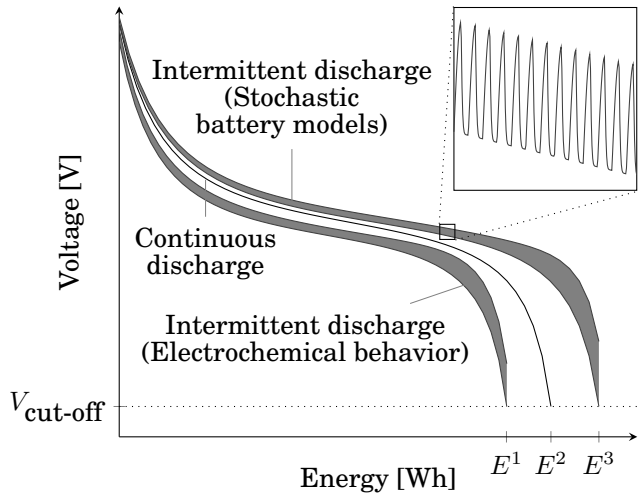

Fig. 1: Motivational example depicting the contradiction between stochastic battery models and electrochemical cell behavior. Stochastic battery models compare unequal intermittent and continuous discharge input patterns (continuous discharge has higher average power than intermittent discharge), which results in a higher energy output[1] E^3 from the battery for an intermittent discharge compared to the energy output E^2 of the continuous discharge. By contrast, the electrochemical cell behavior suggests that a fair, iso-energy input pattern (both continuous and intermittent discharge patterns with equal average power), will provide a reduced energy output E^1 for the intermittent discharge compared to the energy output E^2 of the continuous discharge. This observation is validated by our experimental analysis in Section 5.

1. INTRODUCTION

Recent advancement in the field of wireless communication has enabled the wide-range application of Wireless Sensor Nodes (WSNs) in many real world applications such as environmental monitoring, medical equipment, smart buildings and industrial applications [Pellegrini et al. 2006], [Akyildiz et al. 2002]. WSNs measure the environmental data through various sensors, process it and communicate the data to a base station. Their ability to communicate with other WSNs to form a wireless ad hoc network has enabled the widespread application of these nodes. In general, WSNs are powered using batteries and they are deployed in remote places, having very minimal human interaction. Constant replacement of batteries is not possible in certain applications and therefore it is necessary for these WSNs to maximize their runtime.

Several solutions to increase the runtime of WSNs are available in the literature, ranging from hardware to software level. On the hardware level, optimized circuit designs with low power consumption and techniques to harvest energy from environmental sources such as solar, wind, etc. were proposed. On the other hand, several software techniques such as Dynamic Voltage and Frequency Scaling (DVFS) and Dynamic Power Management (DPM) focus on power saving by turning off inactive resources. Several Media Access Control (MAC) layer protocols and data management techniques have been analyzed in literature to reduce power consumption of WSNs.

A different approach to increase the runtime of WSNs by exploiting nonlinear properties of battery cells, such as the *recovery effect*, has also been considered in the lit-

[1]Here the energy output of the battery is used as a figure of merit to compare intermittent and continuous discharge techniques. The energy output is directly proportional to the runtime of the battery if the battery is discharged in a constant power discharge mode.

erature. There is an existing belief that by performing an intermittent discharge with in-between idle periods, the usable capacity of the battery could be increased because the active materials inside the cell are *self-replenished* and they recover charge during the idle periods [Chiasserini and Rao 2001b]. This concept of recovery effect was explored in literature through stochastic Markov chain models depicting the battery discharge process. The battery recovery effect is modeled as a backward transition edge in the Markov chain battery model [Chiasserini and Rao 2001b]. To exploit the battery recovery effect, several power management techniques in the domain of task scheduling, protocol designs and power supply architectures have been proposed ([Dhanaraj et al. 2005], [Jayashree et al. 2004], [Benini et al. 2001a], [Benini et al. 2001b], [Jongerden et al. 2010]). However, the electrochemical behavior of a cell, as confirmed by our experimental analysis, shows that an intermittent discharge will provide less energy output compared to the continuous discharge of the battery performed with equivalent average power.

Fig. 1 presents a motivating example of this contradiction between stochastic battery models and the electrochemical cell behavior confirmed by our experimental analysis. The stochastic battery models obtain an energy output E^3 by performing an intermittent discharge that consists of a series of T_{ON} and T_{OFF} pulses with a power P_{peak} applied during the T_{ON} period. During the T_{OFF} period, the battery is idled with 0 power applied. This energy output is compared with the continuous discharge of the cell performed with the same peak power P_{peak} and, according to the stochastic battery models, it will provide a reduced energy output E^2 as shown in Fig. 1a. However, this comparison is not fair, since the average power of the intermittent discharge and the continuous discharge is not the same ($P_{\mathrm{avg}}^{\mathrm{intermittent}} < P_{\mathrm{avg}}^{\mathrm{continuous}}$), due to the rest periods (T_{OFF}) in the intermittent discharge pattern. A fair, iso-energy comparison between intermittent and continuous discharge patterns must extract the same amount of energy from the battery, i.e., the average discharge power of the intermittent and continuous discharge patterns must be equal ($P_{\mathrm{avg}}^{\mathrm{intermittent}} = P_{\mathrm{avg}}^{\mathrm{continuous}}$). According to the electrochemical cell behavior confirmed by our experimental results in Section 5, the intermittent discharge provides a reduced energy output E^1 (Fig. 1) compared to continuous discharge for a fair, iso-energy input pattern of intermittent and continuous discharges having equal average power. Until now, neither a clear explanation nor a systematic experimental evaluation of the cell behavior during an intermittent discharge is available. The recovery effect stochastic battery models are not validated with experimental results. In order to analyze the characteristics of the cell during an intermittent discharge and verify the existence of such a battery recovery effect, a systematic evaluation is performed in this paper on real battery cells using a standardized measurement setup.

Contributions and organization of the paper. The major contributions of this paper are as follows:

— For the first time, we developed a standardized evaluation procedure to verify the existence of battery recovery effect and tested three different battery chemistries (alkaline, NiMH and Li-Ion) using a high accuracy battery tester. Our experimental results do not show any evidence of the existence of a battery recovery effect and therefore the existing power management techniques that rely on the recovery effect phenomenon are not usable in practice. All measurement raw data are uploaded in an online repository and made publicly accessible for modeling and verification purposes.
— Moreover, we provide a detailed explanation of why a charge recovery is not possible from an electrochemical perspective. Instead of a charge recovery effect, we identify the *rate capacity effect*, which is defined as the reduction in available battery capacity if the discharge rate is increased, as a dominant electrochemical phenomenon that should be considered for maximizing the battery runtime of WSNs.

— Upon identifying the rate capacity effect as the dominant electrochemical phenomenon, we outline power management techniques to minimize it and increase the runtime of the WSNs.

We provide a comprehensive overview of existing contributions that have utilized the battery recovery effect and proposed different power management techniques in Section 2. In Section 3, we explain an existing stochastic battery model using the recovery effect that is commonly referred in the literature for proposing different power management techniques. We highlight the key points of the model along with the underlying assumptions to the real battery behavior. In addition, we explain in detail the terminologies that are often used in the literature to compare the gain in energy output and runtime extension of the sensor nodes. In Section 4, we present a general block diagram of a typical WSN and discuss the individual modules in detail. We analyze the power supply configurations and the communication modes of the WSN that have an impact on the energy output of the battery based on which we formulate our evaluation procedure in Section 5.

Our proposed evaluation procedure for verifying the existence of the recovery effect in batteries is described in Section 5. Moreover, in this section we provide a detailed analysis of the experimental results obtained from tests performed according to the evaluation procedure using a high accuracy battery tester. Our experimental results do not show any existence of recovery effect, which is a clear deviation from state-of-the-art stochastic battery models. In contrast, our experimental results identify the rate capacity effect as the dominant electrochemical phenomenon which needs to be taken into consideration while designing power management techniques for WSN.

In Section 6, we elucidate the various electrochemical reactions that take place inside the battery during an intermittent discharge. We clearly explain what self-replenishment of active materials inside a battery means from an electrochemical perspective and why a charge recovery effect does not hold in practice. Based on our experimental analysis in Section 5 and the electrochemical explanation of battery behavior in Section 6, in Section 7 we suggest necessary modifications that are required to be made in the existing stochastic models to be used in practice. Moreover, we outline both hardware and software based power management approaches to extend the battery runtime by minimizing the rate capacity effect. Finally, Section 8 summarizes the main findings of the paper and recapitulates our future research directions.

2. RELATED WORK

In this section, existing contributions that analyze, model or exploit the recovery effect behavior of batteries are outlined.

This section is organized into four parts as follows:

— Protocols and design optimization
— Recovery effect models
— Experimental evaluations
— Interpretation of electrochemical literature for power management

Protocols and design optimization. Several works assumed the existence of battery recovery effect and proposed different MAC layer protocols to increase the runtime of the WSN. For example in [Dhanaraj et al. 2005] and [Jayashree et al. 2004], the recovery effect phenomenon is exploited by scheduling the wake-up/sleep time of WSNs appropriately. Communication data traffic control techniques were developed in [Dasika et al. 2004] and [Chiasserini and Rao 2001b] to exploit the recovery effect by optimized discharge profiles of the battery. Similar scheduling algorithms are proposed in [Chenfu et al. 2015] in the area of wireless body sensors, where an improvement of 70 % is reported by exploiting the battery recovery effect. On the other hand, multiple-battery power supply architectures and battery scheduling schemes are proposed in [Benini et al. 2001a], [Benini et al. 2001b] to exploit the battery recovery effect. In [Chiasserini and Rao 2001a], [Jongerden et al. 2010], scheduling algorithms are proposed to exploit the recovery effect phenomenon by switching between batteries

to draw power in a multi-battery power supply architecture. They claim that scheduling between the batteries to draw power provides longer runtime compared to the constant parallel-connected battery power supply architecture because of the charge recovery effect. However, all the above mentioned works do not evaluate or prove the existence of the battery recovery effect, but they rely on stochastic battery models from literature using recovery effect as a basis of their work.

Stochastic battery models. Several stochastic models for the battery recovery effect are available in literature. A consolidation of various battery models is presented in [Jongerden and Haverkort 2009]. In [Chiasserini and Rao 1999a], [Chiasserini and Rao 1999b] and [Sarkar and Adamou 2003] the dynamics of cell behavior for an intermittent discharge current profile were captured using a Markov chain model. Similarly, [Rong and Pedram 2006] proposed a continuous-time Markovian decision processes for modeling the recovery effect behavior of the battery. Although the methodology for shaping the communication data traffic using the above mentioned battery models is valid, the underlying assumption of charge recovery in these models is not formalized. Instead of proving the existence of the charge recovery, these models assume that a battery recovers charge when it is allowed to rest. A detailed explanation of a commonly used stochastic battery models using recovery effect is presented in Section 3.1.

Experimental evaluations. Another class of work focuses on verifying the existence of the recovery effect by performing experimental tests on battery cells. In [Castillo et al. 2004], a relay switch controlled by a computer is used to perform intermittent and continuous discharge experiments on four different battery chemistries (alkaline, Nickel Cadmium (Ni-Cd), NiMH and Li-Ion) to verify the existence of recovery effect. Their results indicate that the recovery effect is only prevalent in alkaline cell chemistry, whereas the other battery types did not show any charge recovery effect. Moreover, in [Chau et al. 2010], two commercial WSNs were used to generate discharge patterns with varying active/sleep durations, on a standard $600\,\mathrm{mA\,h}$ NiMH cell. With intermittent discharge, an increase of 30 to 45% of normalized battery runtime compared to a continuous discharge was reported. Both of the above-mentioned works compare the *normalized runtime* of an intermittent discharge test with the total runtime of the continuous discharge test for proving the existence of the battery recovery effect. Fig. 2 better explains the implications of this comparison. Existing works perform intermittent discharge experiments with the test pattern shown in Fig. 2a, in which the battery is discharged with a power P_{pulse} for a time period T_{ON} followed by a rest period of T_{OFF} with 0 power applied. The *normalized runtime* of this test pattern, sum of T_{ON}, till the battery is fully discharged is compared with the total runtime of the continuous discharge shown in Fig. 2b, where the battery is discharged with the same peak power P_{pulse}. This comparison is unfair since the discharge pattern shown in Fig. 2b has a higher average value than the discharge pattern in Fig. 2a, due to the rest periods T_{OFF} in the later case. Conversely, comparing the total runtime of the continuous discharge pattern shown in Fig. 2c with the *normalized runtime* obtained from Fig. 2a will lead to a fair comparison. An even fairer analysis for verifying the existence of the battery recovery effect involves comparing intermittent discharge tests performed with different values of T_{ON} and T_{OFF}. In Section 5, we developed an evaluation procedure considering different ratios of T_{ON} and T_{OFF} for an intermittent discharge, to verify the existence of battery recovery effect. More explanation regarding the normalized runtime and its effect on estimating the total battery capacity is presented in Section 3.2.

Interpretation of electrochemical literature for power management. There are several works in the electrochemical domain that explain the benefits of an intermittent discharge in certain battery chemistries. For example, [LaFollette 1995] and [Nelson et al. 1997] explain the design and development of a novel battery based on lead-acid chemistry that is capable of withstanding high pulse power. Both the above-mentioned works explain a well-known electrochemical behavior of lead-acid battery chemistry towards intermittent discharge. Even though lead-acid cells show an improved performance with an intermittent load, due to their huge size and weight, they

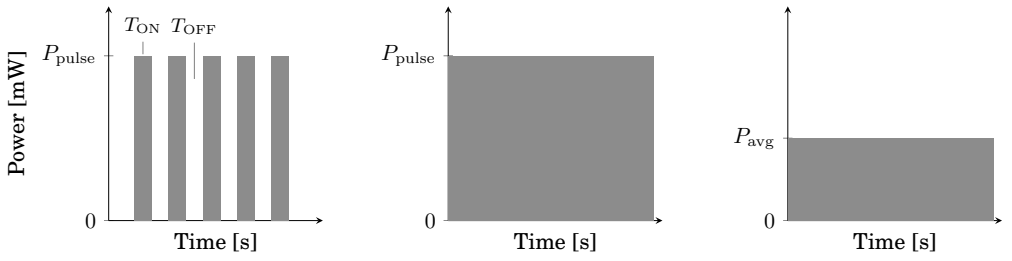

(a) Intermittent discharge (b) Continuous discharge with peak power (c) Continuous discharge with average power

Fig. 2: Intermittent and continuous discharge patterns. (a) Intermittent discharge with peak power P_{pulse} applied during T_{ON} and 0 power applied during T_{OFF}. (b) Continuous discharge with same peak power (P_{pulse}) of the intermittent discharge in (a). (c) Continuous discharge with average power P_{avg} of the intermittent discharge in (a).

are not generally used as power supply for WSN applications. However, this specific behavior of lead-acid cells has been generalized to other battery chemistries in certain literature as explained previously in this section. Based on this incorrect generalization, several stochastic Markov chain battery models and power management techniques have been proposed. Furthermore, the basis for the chemical explanation of the recovery effect in most existing contributions is primarily based on [Fuller et al. 1994], where the voltage relaxation phenomena (the relaxation of the cell voltage towards equilibrium after a charge or discharge pulse) in lithium-ion-insertion cells was discussed. While this paper does not mention any form of recovery effect, it has been incorrectly cited as a reference for the existence of recovery effect by the stochastic battery models mentioned in this section.

Summary. In summary, several power management techniques in the form of communication data scheduling and power supply architecture are available in the literature. However, these works are based on stochastic battery models that are not experimentally validated and assume that a battery recovers charge when it is allowed to rest. Moreover, the results from discharge experiments performed in the literature are misinterpreted and claim the existence of the recovery effect. In addition, the well-known findings in the electrochemical sources pertaining to a specific battery chemistry are generalized to other battery chemistries and used as a source for the existence of the recovery effect. Therefore, in this paper, we perform a systematic experimental evaluation on real battery cells using a standardized measurement setup for evaluating the benefits in terms of energy output obtained from an intermittent discharge compared to a continuous discharge.

3. MODELS AND TERMINOLOGIES

In this section, we explain a stochastic battery discharge model using recovery effect that is commonly referred in power management literature. Later, we again discuss this model in conjunction with our experimental evaluations, in order to understand which aspect of the model deviates from our experimental results. We then further, in Section 7, update this model so that it confirms to our experimental results, in which case the model gets transformed into a battery discharge model and no longer shows any recovery effect. In addition, we provide a detailed explanation on *normalized runtime* of an intermittent discharge, which is used to calculate the gain in runtime obtained due to recovery effect.

3.1. Existing Stochastic Battery Model Using Recovery Effect

Fig. 3, shows an existing stochastic battery discharge model using recovery effect as proposed in [Chiasserini and Rao 2001b], which is widely utilized ([Chowdhury and

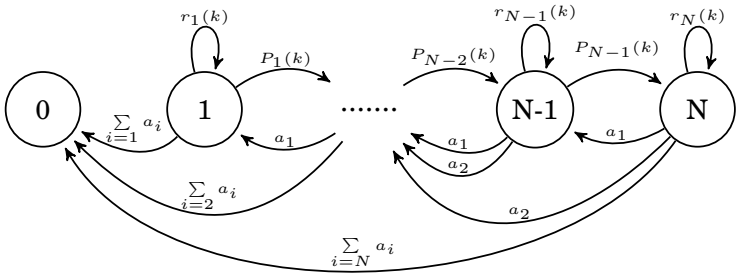

Fig. 3: Markov chain model of a battery discharge process capturing the recovery effect behavior [Chiasserini and Rao 2001b].

Chakrabarti 2005], [Nuggehalli et al. 2006]) for shaping communication data traffic in WSNs. The battery discharge process is represented in states N, $N-1$,..., 0. The basic amount of charge that is drained from a cell in one time slot is defined as one *charge unit*. Each fully charged cell is assumed to have a theoretical capacity equal to T charge units and a nominal capacity equal to N charge units. The nominal capacity represents the charge that could be drawn from the cell using a continuous discharge and it is less than the theoretical capacity.

The fully charged state of the cell is N and state 0 represents the completely discharged state of the cell. The cell discharge is depicted as a stochastic process as shown in Fig. 3, that starts from state N and terminates either when state 0 is reached or the theoretical capacity T is exhausted. Therefore, in each time slot depending upon the communication data packet arrival, the cell discharges i charge units to process the data and move from state z to state $z-i$ with $i < z \leq N$. The probability for a data packet to arrive in a time slot is defined as a_i.

During the rest periods of an intermittent discharge, the cell shall remain in the same state or recover one charge unit as shown in Fig. 3 depending upon the probability $P_j(k)$ given by:

$$P_j(k) = \begin{cases} a_0 e^{-(N-j)\alpha_N - \alpha_C(k)}, & \begin{array}{l} j = 1, ..., N-1 \\ k = 0, ..., \Gamma_1 \end{array} \\ a_0 e^{-(N-j)\alpha_N - \Gamma\alpha_C(k)}, & \begin{array}{l} j = 1, ..., N-1 \\ \Gamma_c \leq k \leq \Gamma_{c+1} \\ c = 1, ..., c_{max} - 1 \end{array} \end{cases}$$

with c_{max} being the number of discharge phases, $\Gamma_{c_{max}} = T$ and α_N, α_C depends upon the recovery capability of the battery. The probability to recover charge is modeled as a decreasing exponential function of the cell State-of-Charge (SoC), since the ability to recover charge decreases at low SoC values and the exponential decay coefficient (α_N, α_C) takes different values depending upon the discharge capacity [Chiasserini and Rao 2001b]. On the other hand, the probability to remain in the same state is defined as:

$$r_j(k) = a_0 - P_j(k), \; j = 1, ..., N-1; \quad k = 0, ..., T$$

$$r_N(k) = a_0, \qquad\qquad k = 0, ..., T$$

The gain in runtime due to battery recovery effect is calculated as:

$$G = \frac{\overline{m}_p}{N} \tag{1}$$

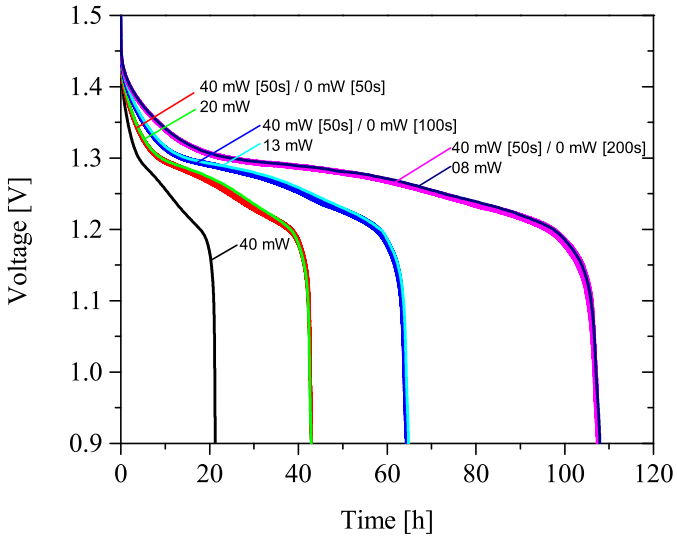

Fig. 4: Measured runtime of a commercial NiMH cell for different $T_{\mathrm{ON}}/T_{\mathrm{OFF}}$ ratios of intermittent discharge and continuous discharge at equivalent average power.

with $\overline{m}_p$ being the average number of charge units drained from the cell with an intermittent discharge and N is the average number of charge units discharged by the cell from a continuous discharge. The model is simulated with different data packet arrival processes such as Bernoulli-driven discharge demand and truncated Poisson distribution and the results in [Chiasserini and Rao 2001b] show that the gain due to recovery effect is more pronounced for a burst packet transmission process, since the idle time is more in a burst transmission compared to the periodic data transmission.

This observation is due to the edges $P_j(k)$ in Fig. 3, which indicates that irrespective of the battery chemistry, if a battery is allowed to rest after a pulse, the active materials inside the battery are *self-replenished* due to the diffusion process and recover charge. This assumption is also used to model the recovery effect as a battery transition system in [Boker et al. 2014]. In contrast to these results, [Rao et al. 2005] observed that the battery-aware task scheduling techniques considering the recovery effect phenomenon, are ineffective compared to the energy optimization techniques, that focus only on optimizing the actual charge that is delivered to the load by the battery. While their observation holds for both very fine-grained (less than 10 ms) and very coarse-grained tasks (greater than 30 min), it is based on an alternative interpretation of the high-level battery model from [Rakhmatov and Vrudhula 2003]. However, both the existence of these recovery edges and the findings in [Rao et al. 2005] in a real battery behavior are not experimentally validated or explained from an electrochemical perspective.

Our experimental evaluations in Section 5 characterize the battery behavior during an intermittent discharge and show that the energy output obtained from an intermittent discharge is less when compared to the energy output obtained from a continuous discharge. This is a clear contradiction to the assumption of the existence of charge recovery edges by the stochastic models. Furthermore, we will explain in Section 6 what self-replenishment of active materials inside the battery implies and why such self-replenishment is not feasible from an electrochemical perspective.

3.2. Normalized Runtime of an Intermittent Discharge

In this section, we explain what a *normalized runtime* of an intermittent discharge means and why comparing it with the total runtime of a continuous discharge is not valid.

A single pulse of an intermittent discharge is characterized by an active period T_{ON} during which the cell is discharged with a peak power P_{pulse}, followed by a rest period T_{OFF} during which no power is applied as shown in Fig. 2a. The *normalized runtime* for this discharge pattern is calculated as follows ([Chau et al. 2010]):

$$\text{Normalized runtime} = T_{\mathrm{pulse}} \cdot \frac{T_{\mathrm{ON}}}{T_{\mathrm{ON}} + T_{\mathrm{OFF}}} \tag{2}$$

with T_{pulse} being the measured total battery runtime of the intermittent discharge pattern shown in Fig. 2a and the ratio of $\frac{T_{\mathrm{ON}}}{T_{\mathrm{ON}}+T_{\mathrm{OFF}}}$ is called as duty-cycle rate of an intermittent discharge. Fig. 2b shows a continuous discharge of a battery performed with the same peak power P_{pulse} of the intermittent discharge, which provides a total battery runtime of T_{cont}. In [Chau et al. 2010], the *normalized runtime* calculated as per the Eq. (2) is compared with the total runtime (T_{cont}) obtained from the continuous discharge test performed with the same peak power of the intermittent discharge. This is not a valid comparison because the average power drawn from the battery cell in the intermittent discharge case is reduced by the rest periods (T_{OFF}). On the other hand, the total runtime (T_{pulse}) of the intermittent discharge performed with peak power P_{pulse} must be compared with the total runtime (T_{avg}) of the continuous discharge (shown in Fig. 2c) performed with equivalent average power P_{avg} computed as follows:

$$P_{\mathrm{avg}} = P_{\mathrm{pulse}} \cdot \frac{T_{\mathrm{ON}}}{T_{\mathrm{ON}} + T_{\mathrm{OFF}}} \tag{3}$$

with P_{pulse}, T_{ON} and T_{OFF} being the peak power, active and rest periods of the intermittent discharge, respectively. For example, an intermittent discharge with T_{ON} = T_{OFF} = $50\,\mathrm{s}$ and a peak power (P_{pulse}) of $40\,\mathrm{mW}$ has an average power (P_{avg}) of $20\,\mathrm{mW}$ as per Eq. (3). Therefore, comparing the *normalized runtime* of the intermittent discharge (Fig. 2a) with the total runtime of the continuous discharge performed with same peak power (Fig. 2b) results in an overestimation of the battery capacity. Instead, the total runtime of the intermittent discharge has to be compared with the total runtime of the continuous discharge performed with equivalent average power (Fig. 2c). This is experimentally verified in Fig. 4 for the case of a commercial NiMH cell with different values of T_{ON} and T_{OFF} for intermittent discharge and corresponding continuous discharge tests performed with equivalent average power.

4. ARCHITECTURE AND OPERATING MODES OF WSN

In this section, a detailed analysis of the building blocks of a WSN and their existing power management approaches are presented. Understanding the WSN architecture and its working behavior enables to analyze the impact on the energy output obtained from the battery. Moreover, it facilitates to clearly interpret our evaluation procedure and results explained in Section 5 for experimentally analyzing the existence of the battery recovery effect. For example, the test patterns in Sets 1, 2 and 3 described in Table I (Section 5 on page 13) are equivalent to periodically switching the batteries to power the WSN in a multiple-battery setup as explained in Section 4.2. Comparing the results of these tests with the output of Set 4 in Table I corresponds to evaluating the different power supply configurations shown in Fig. 6. Similarly, the different communication patterns (periodic vs. burst) of WSNs explained in Section 4.2, are evaluated by comparing the output of tests with equal $(T_{\mathrm{ON}}/T_{\mathrm{OFF}})$ in Sets 1, 2 and 3 described in Table I. Therefore, a detailed explanation regarding the different operating modes of the WSN is required to understand our experimental setup and results explained in Section 5.

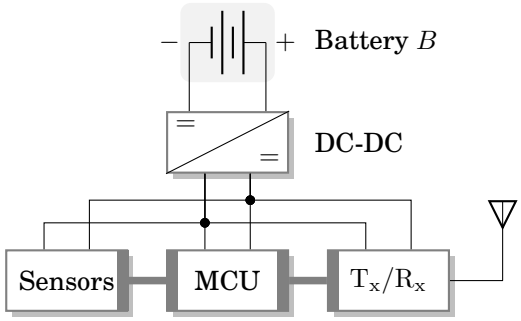

Fig. 5: Functional block diagram of a typical WSN [Raghunathan et al. 2002]. Measured sensor data is processed by the MCU and transmitted through the transceiver. The DC-DC converter provides a constant regulated power from the battery B.

4.1. Architecture of a WSN

The general architecture of a typical WSN is shown in Fig. 5 and can be classified into four modules as:

— Sensing module
— Computation module
— Communication module
— Power supply module

Sensing module. The sensing module consists of different types of sensors which establish connection between the WSN and the environment. They could be classified as either passive sensors such as temperature and humidity, which consume less power, or active sensors such as image recorders and Global Positioning System (GPS), which are large power consumers. Turning off sensors during inactive periods reduces their power consumption and enables them to achieve longer battery runtime.
Computation module. The computation module consists of the MCU, which controls all other blocks in the WSN. It receives input data from the sensing module, processes it and transmits the information through the communication module. Different power saving techniques such as DPM, DVFS exist in literature [Choi and Cha 2010] to reduce the power consumption in MCUs. Most MCUs provide low power modes of operation to reduce the power consumption of the WSN during sleep state.
Communication module. The communication module consists of the wireless radio which enables the communication between other WSNs or to the base station. Power savings in wireless radios can be done by duty cycling their operation with appropriate wake-up and sleep times. Several communication protocols such as ASLEEP [Anastasi et al. 2009], S-MAC [Ye et al. 2004], B-MAC [Polastre et al. 2004] and DS-MAC [Peng et al. 2004] allow duty cycling of the wireless radio in order to reduce the energy consumption. On the other hand, in-network data processing techniques such as data compression or data aggregation [Mo et al. 2011] and energy efficient communication data routing mechanisms as in [Junyoung et al. 2009] help to reduce the energy consumption of the wireless radio.
Power supply module. The power supply module is comprised of the battery and the DC-DC converter. The DC-DC converter provides constant regulated power for the operation of other WSN modules. The converter could be either step-up (Boost), step-down (Buck or Linear) or step-up/down (Buck-boost) converter [Erickson and Maksimovic 2001]. From a system designer's point of view, most batteries are considered as a black box, providing constant voltage until their end-of-life. In contrast to this, the output voltage of most batteries declines continuously with discharge. In such cases, a DC-DC converter plays a vital role by providing constant regulated supply voltage taking into consideration the decreasing battery output voltage [Min et al. 2001], [Sinha and

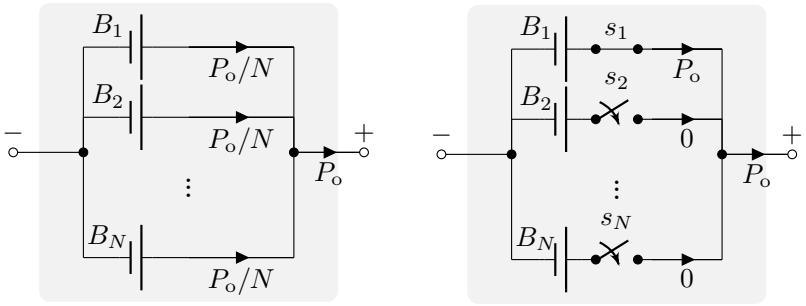

(a) Parallel configuration (b) Switching configuration

Fig. 6: Multiple battery power supply architectures for WSNs. (a) Cells are connected in parallel to share the power delivered to the WSN, configuration A. (b) Cells are periodically switched to provide power to the WSN, configuration B.

Chandrakasan 2001] and [Benini et al. 2003]. In general, it is a popular belief among most designers that adding a DC-DC converter will reduce the overall efficiency of the system due to the internal losses in the converter. However, it was experimentally proven in [Day 2009] that by adding a DC-DC converter there could be a significant increase in the battery runtime, even after considering internal losses of the converter. Two systems (system 1 and system 2) were experimentally verified in [Day 2009] to analyze benefits of powering a MCU (MSP430FG4168) with a DC-DC converter. In system 1, the MCU was powered directly from two series-connected AA alkaline cells. In system 2, a DC-DC converter (TPS780xx) was used to provide a constant supply voltage of $2.2\,\mathrm{V}$ to power the MCU from the battery. At the end of the experiment, system 2 with the DC-DC converter operated for 298 hours, whereas system 1 operated for a duration of 233 hours. An increased runtime of 30% was achieved, even after considering efficiency losses of the DC-DC converter. This is due to the fact that the current consumption of a typical MCU increases linearly with the supply voltage and therefore the MCU in system 1 (which is directly powered from the battery) consumed higher currents initially when the battery was fully charged. However, in system 2, the DC-DC converter maintained a constant $2.2\,\mathrm{V}$ supply voltage, thereby reducing the current consumption of the MCU compared to system 1.

Implications of DC-DC converter on our experiments. The addition of a DC-DC converter modifies the discharge profile of the battery by increasing the current drawn at lower cell voltage to maintain a constant power. As a result, the battery is discharged with constant power. Hence, all our experiments in Section 5 are performed with constant power discharge mode in order to make the results reproducible for most WSN and portable computer applications. In applications where a DC-DC converter is not involved, the magnitude of the discharge current is proportional to the supply voltage and it behaves like a constant resistance load to the battery.

4.2. Power Supply Configurations and Communication Modes

In this section, we analyze two power supply configurations (constant parallel-connected and switched) that have an impact on the energy delivered to the system. Moreover, we discuss two different communication modes (periodic and burst transmission) of the WSN, in case of single battery powered applications. Based on these two test cases, we formulate an evaluation procedure in Section 5 to verify the existence of battery recovery effect.

Power supply configurations. In applications where weight or size of the WSN is not a critical parameter, more than one battery cell can be used as power supply as shown in Fig. 6. Implementations using multiple batteries as power supply are explored extensively in the literature [Dhanaraj et al. 2005], [Benini et al. 2001b], [Chi-

asserini and Rao 2001a], [Qing et al. 2000], [Lahiri et al. 2002]. It is claimed in the literature that periodically switching between the batteries to power the WSN as shown in Fig. 6b provides a gain in runtime due to the recovery effect compared to the constant parallel-connected setup shown in Fig. 6a. However, this claim is only based on stochastic battery models explained in Section 3 and no experimental evaluation was performed on batteries considering a multiple battery setup. In Fig. 6a, hereafter referred to as configuration A, cells of equal capacity are connected in parallel and the input power required by the WSN is shared equally by all of them. If P_{o} is the power required by the WSN, then the power delivered by individual cells P_i is given by

$$P_i = \frac{P_{\mathrm{o}}}{N} \tag{4}$$

with N being the number of cells connected in parallel. In Fig. 6b, hereafter referred to as configuration B, cells are periodically switched to power the WSN. Therefore, pulses of power P_{o} are periodically drawn from each cell with a certain rest period. This operation mode is experimentally analyzed in Section 5.

Communication modes. In general, WSNs are operated in sleep mode for most of the time to reduce the energy consumption from the battery. They are periodically woken up to transmit the processed data or process the received data. The average end-to-end power consumption of a wireless radio is [Shih et al. 2004]:

$$\begin{aligned} P_{\mathrm{radio}} =& N_{\mathrm{tx}}[P_{\mathrm{tx}}(T_{\mathrm{on-tx}} + T_{\mathrm{st}}) + P_{\mathrm{out}} \cdot T_{\mathrm{on-tx}}] + P_{\mathrm{bb-tx}} \\ &+ N_{\mathrm{rx}}[P_{\mathrm{rx}}(T_{\mathrm{on-rx}} + T_{\mathrm{st}})] + P_{\mathrm{bb-rx}} \end{aligned} \tag{5}$$

with $N_{\mathrm{tx/rx}}$ being the average number of times per second the transceiver is used, $P_{\mathrm{tx/rx}}$ is the power consumption of the transceiver, P_{out} is the output transmit power, $T_{\mathrm{on-tx/rx}}$ is the on-time of the transceiver, T_{st} is the start-up time of the transceiver and $P_{\mathrm{bb-tx/rx}}$ is the average power consumption of the baseband block.

Every transceiver (transmitter and receiver) device has a nonzero start-up time (T_{st}) during which no data is transmitted or received. Power consumption of the wireless radio at low data rates is dominated by the power consumption during this start-up period of the transceiver. Therefore, the wake-up/sleep time of the WSN ($T_{\mathrm{on-tx/rx}}$) has to be chosen appropriately, considering the packet size to minimize start-up transient losses in the transceiver. The WSN can either transmit the processed data periodically as shown in Fig. 7a or buffer the data and transmit it as a burst (Fig. 7b). It is claimed in literature that by allowing the battery to rest long enough during an intermittent discharge (as in burst transfer mode), the total runtime of the battery is increased due to charge recovery effect. To investigate the effect of both operating scenarios on batteries, experiments were performed in Section 5, with different periods of ON and OFF times ranging from $0.5\,\mathrm{s}$ to $50\,\mathrm{s}$.

5. EVALUATION PROCEDURE AND RESULT ANALYSIS

In this section, we present the systematic evaluation procedure formulated to verify the battery recovery effect. A detailed overview of the high accuracy battery tester used to implement our evaluation procedure is provided. As already mentioned before, the results obtained from our experimental evaluations do not show any evidence for existence of recovery effect. By contrast, our results show that the rate capacity effect to be the dominant electrochemical phenomenon that should be considered for developing power management techniques for WSNs.

5.1. Evaluation Procedure

The systematic evaluation procedure shown in Table I enables to experimentally verify the recovery effect behavior on batteries under different discharge load patterns. Sets 1 to 3 consist of intermittent discharge tests with different values of T_{ON}, T_{OFF} and Set 4 represents the corresponding continuous discharge tests performed with equivalent average power of intermittent discharge computed according to Eq. (3). T_{ON} and T_{OFF}

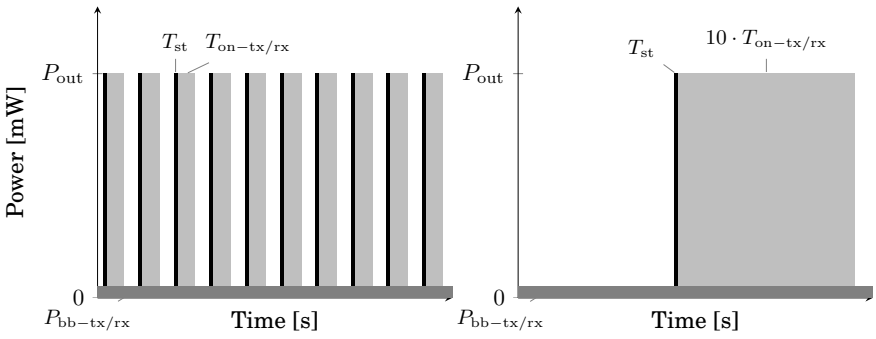

(a) Periodic transfer (b) Burst transfer

Fig. 7: Power consumption of a WSN during communication. (a) Periodic data transfers with start-up power at the beginning of every transmission. (b) Burst data transfer where the start-up power is required for a single time.

represent active and sleep states of the WSN, respectively. The discharge power value shown in Table I was only applied to the cell during T_{ON} period and during T_{OFF} period the cell was completely isolated, with zero power applied. The operating voltage of most commonly used WSNs (TelosB, TMote [Werner et al. 2006] and Mica Motes [Horton et al. 2002]) are in the range of $3.3\,\text{V}$ and their overall current consumption is around $25\,\text{mA}$. Therefore, a power consumption value of $80\,\text{mW}$ was chosen upon multiplying the operating voltage and the total nominal current consumption of these WSNs. In addition, the batteries used in these nodes are either two series-connected alkaline or NiMH cells, or a single Li-Ion cell. Therefore, the discharge power was halved in case of tests performed with alkaline and NiMH cells and full discharge power was applied in case of Li-Ion cells, since single cells were used for our experimental analysis. Moreover, the active and sleep periods in WSNs can vary widely depending upon the application scenario. For example, in environment monitoring applications the T_{OFF} periods could be very large ranging from minutes to hours. Therefore, in our evaluation procedure we have considered a wide spread of T_{ON} and T_{OFF} values as shown in Table I.

	T_{ON}[s]	T_{OFF}[s]	$T_{\text{ON}}/T_{\text{OFF}}$	Power at T_{ON}[mW]	
				Alkaline & NiMH	Li-Ion
Set 1	50	50	1:1	40	80
	50	100	1:2		
	50	200	1:4		
Set 2	5	5	1:1	40	80
	5	10	1:2		
	5	20	1:4		
Set 3	0.5	0.5	1:1	40	80
	0.5	1	1:2		
	0.5	2	1:4		
Set 4	Continuous			20	40
				13.3	26.6
				8	16

Table I: Evaluation procedure for verifying the existence of the battery recovery effect in WSN applications. Set 1, 2, 3 are intermittent discharge tests with different values of T_{ON} and T_{OFF} and Set 4 is the corresponding continuous discharge test with equivalent average power.

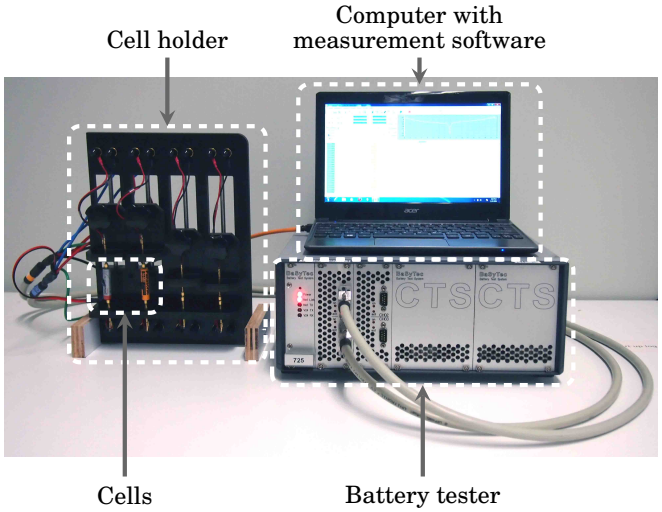

Fig. 8: BaSyTec CTS battery tester setup along with a computer running the measurement software for the systematic experimental evaluation of the battery recovery effect.

Energy output of all tests was recorded to evaluate the existence of battery recovery effect. The energy output of the battery is directly proportional to the runtime since the battery is discharged in a constant power discharge mode.

Verification of power supply configurations. The multiple-battery power supply architectures explained in Section 4.2 are experimentally verified using the evaluation procedure in Table I. By comparing the energy output obtained from intermittent discharge tests performed in Sets 1, 2 and 3 to the energy output obtained from continuous discharge tests done in Set 4, the effectiveness of the two power supply configurations could be experimentally evaluated. For example, the test done in Set 4 with a continuous power discharge of 8 mW is equivalent to configuration A, shown in Fig. 6a with $N = 5$. Similarly, the test performed in Set 1 with T_{ON} = 50 s and T_{OFF} = 200 s is equivalent to configuration B, shown in Fig. 6b with $N = 5$. By comparing the energy output of the battery obtained from both tests, an analysis of which power supply architecture provides higher energy output for $N = 5$ could be performed and thereby the existence of recovery effect in a multiple-battery setup could be experimentally verified. Similar comparisons could be made for $N = 2$ and $N = 3$ from tests performed with different ratios of T_{ON} and T_{OFF} according to Table I.

Verification of communication modes. The effect of varying the wake-up/sleep time of the WSN on batteries as explained in Section 4.2 is experimentally verified by comparing the energy output obtained from tests done with equal $T_{\mathrm{ON}}/T_{\mathrm{OFF}}$ ratios in all sets from Set 1 to 3. For example, the test performed in Set 3 with T_{ON} = T_{OFF} = 0.5 s is equivalent to a periodic transmission of data as shown in Fig. 7a. Correspondingly, the test case T_{ON} = T_{OFF} = 5 s in Set 2 is equivalent to the WSN buffering the input data and transmitting it in bursts, as shown in Fig. 7b. For a qualitative comparison between periodic data transfer mode and burst data transfer mode, the start-up time (T_{st}) of the transceiver and the baseband power ($P_{\mathrm{bb-tx/rx}}$) are not considered in the evaluation procedure. However, for optimization of the data packet size to minimize energy consumption, start-up time and baseband power should be taken into account. By comparing the energy output obtained from these tests, the influence of varying wake-up/sleep times of the WSN on the battery power supply could be experimentally analyzed.

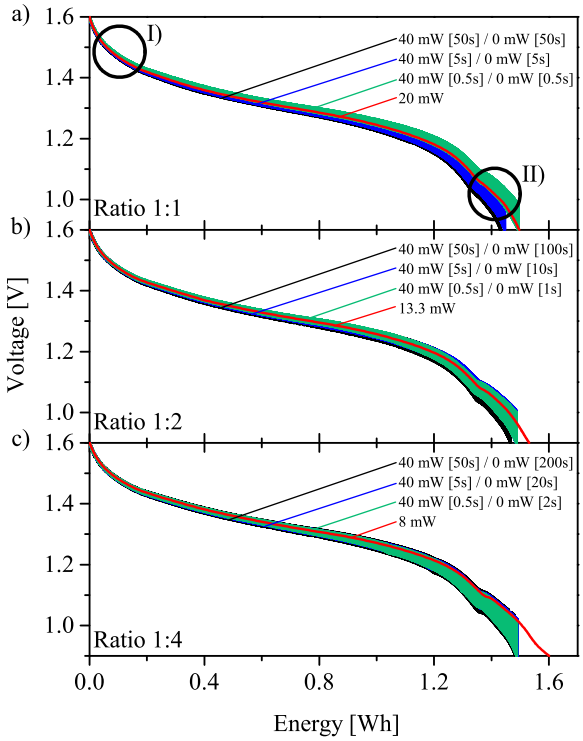

Fig. 9: Continuous and intermittent discharge of the alkaline batteries with $(T_{\mathrm{ON}}/T_{\mathrm{OFF}})$ ratio of (a) 1:1, (b) 1:2 and (c) 1:4. Discharge powers are indicated along with T_{ON} and T_{OFF} times in square brackets.

Table II: Energy output obtained from alkaline battery with our evaluation procedure.

Power in mW [Time in s]	Energy Output [Wh]
40 [50] / 0 [50]	1.43
40 [5] / 0 [5]	1.44
40 [0.5] / 0 [0.5]	1.49
20	1.5
40 [50] / 0 [100]	1.46
40 [5] / 0 [10]	1.48
40 [0.5] / 0 [1]	1.486
13.3	1.53
40 [50] / 0 [200]	1.48
40 [5] / 0 [20]	1.49
40 [0.5] / 0 [2]	1.487
8	1.6

5.2. Battery Tester

All tests listed in Table I were performed using a high accuracy BaSyTec CTS battery tester (BaSyTec GmbH, Germany) [BaSyTec Tester 2013]. The BaSyTec CTS system is capable of accurately characterizing battery cells up to a maximum charge and discharge current of $5\,\mathrm{A}$. Advantages of this tester are the precise control of applied power or current, high accuracy, high resolution measurements and fast data acquisition of current, voltage, temperature and time. Furthermore, the implementation of various test cases is easy and flexible, reducing the risk of unforeseen human errors. An example test setup is shown in Fig. 8, containing a 4-channel BaSyTec CTS battery tester, a notebook running the measurement software and the cell holder containing the cells.

5.3. Analysis of Experimental Results

In this section, experimental results from our evaluation procedure of the recovery effect are presented and analyzed. All tests were performed on three different commercially available battery chemistries (alkaline, NiMH and Li-Ion), that are suitable power sources for WSN applications. Results of each individual chemistry are plotted separately and explained in the remainder of this section.

All cells were discharged according to the evaluation procedure in Table I, until their voltage reached the cut-off value, specified in their data sheet. In order to detect possible manufacturing variances, all tests were performed on two cells of the same batch.

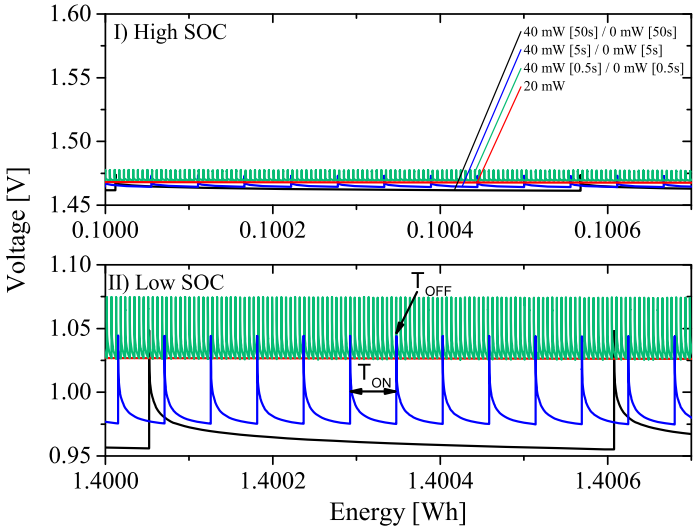

Fig. 10: Magnification of the discharge profile shown in Figure 9a at a high SoC (I) and low SoC (II).

The maximum detected variance between two cells for the same test pattern was in the range of 1.5%. Data was recorded in the BaSyTec measurement software for a step change of 1 mV in battery voltage. All measurement raw data of approximately 5 GB of size is available for reference and modeling purposes at [Recovery Effect Results 2015].

Alkaline battery. AAA alkaline batteries from Varta (powerone) [Varta Alkaline 2003] were used for our evaluation. Energy output obtained from various ratios of $(T_{\mathrm{ON}}/T_{\mathrm{OFF}})$ is plotted in Fig. 9, where Fig. 9 a, b and c correspond to $(T_{\mathrm{ON}}/T_{\mathrm{OFF}})$ ratios of 1:1, 1:2 and 1:4, respectively. Values of T_{ON} and T_{OFF} along with their corresponding discharge power are indicated in the graph and explained in Table I. The figure also includes the energy output obtained from the continuous discharge tests performed with equivalent average power for each specified $(T_{\mathrm{ON}}/T_{\mathrm{OFF}})$ ratio. All tests were performed until the cell voltages reached their cut-off values of 0.9 V as specified in their datasheet. The energy output obtained from the battery for each test case is provided in Table II.

Fig. 10 shows the magnification of the discharge profile of Fig. 9a at two specific SoC regions (high and low). At high SoC values, the difference in cell voltage between T_{ON} and T_{OFF} of an intermittent discharge is less compared to that at low SoC values. As a result, the cell voltage profile becomes broader towards the end of discharge. Due to the high sampling rate of the tester, the cell voltage looks like a thick broad line at low SoC values in Fig. 9. From our experimental results for alkaline cells shown in Table II, we observe that the energy output obtained from intermittent discharge tests for different values of T_{ON} and T_{OFF} is less compared to the energy output obtained from continuous discharge tests performed with equivalent average power. This indicates that there is no existence of charge recovery effect and therefore the existing power management techniques that rely on the recovery effect phenomenon are not applicable in practice. Based on this observation, in Section 7.1 we provide necessary amendments for the existing stochastic battery models that rely on the recovery effect.

From Table II, the energy output obtained from continuous discharge tests of 8 mW and 20 mW are 1.6 W h and 1.5 W h, respectively. Even at these investigated lower

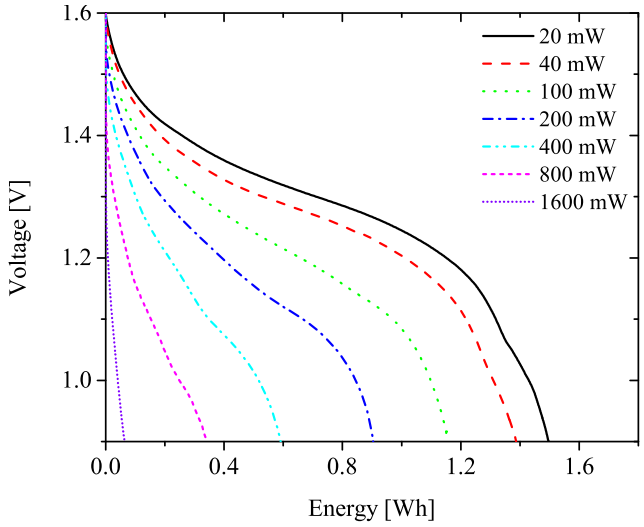

Fig. 11: Discharge profiles of alkaline batteries measured at different constant power rates as indicated. A higher power rate reduces the usable energy output of the cell.

power rates, we observe a significant change in the energy output obtained from the battery. This is primarily attributed to the rate capacity effect, which states that increasing the rate of discharge decreases the capacity and energy output obtained from the battery (a detailed explanation of the rate capacity effect is provided in Section 6). The rate capacity effect can be observed from the measurements shown in Fig. 11, where higher energy output can be obtained by discharging the cell at lower discharge powers. Therefore, from our experimental analysis on alkaline cells, we identify that the rate capacity effect to be the dominant electrochemical phenomenon governing the energy output obtained from the battery. Henceforth, in Section 7.2, we outline hardware and software based power management techniques to obtain higher energy output from the battery by minimizing the rate capacity effect.

NiMH and Li-Ion batteries. Results for NiMH (Panasonic, HHR-75AAA/HT) [Panasonic NiMH 2000] and Li-Ion (GSP062530) [GSP Li-Ion 2012] cells for $(T_{\mathrm{ON}}/T_{\mathrm{OFF}})$ ratio of 1:1 are shown in Fig. 12a and 12b, respectively. The cut-off voltage of NiMH cells is $0.9\,\mathrm{V}$ and the cut-off voltage of the investigated Li-Ion cell is $3\,\mathrm{V}$. For both battery chemistries no change in energy output was observed for intermittent and continuous discharge tests performed as per Table I. The discharge profiles of $(T_{\mathrm{ON}}/T_{\mathrm{OFF}})$ ratios 1:2 and 1:4 did not show any variation and therefore are not included here, whereas the measurement data is available in the online repository [Recovery Effect Results 2015]. In comparison to the alkaline cells, the experimental results of NiMH and Li-Ion batteries as shown in Fig. 12a and 12b, respectively, do not show any significant deviation in energy output between continuous discharge tests and intermittent discharge tests for various $(T_{\mathrm{ON}}/T_{\mathrm{OFF}})$ values. The reason for this behavior is that the designs of the NiMH and Li-Ion cells are capable of withstanding higher power rates than those commonly experienced in commercial WSN applications. Therefore, they do not show a significant rate capacity effect in the investigated power range mentioned in Table I. Nevertheless, $30\,\%$ to $40\,\%$ improvements obtained in energy output due to intermittent discharges, as claimed by existing works referenced in Section 2, are in clear contradiction with our experimental results. Small variations in the energy output observed are primarily attributed to manufacturing variances of cells and ambient temperature fluctuations of $\pm$ 3 °C during the experiment. Therefore, in these battery chemistries,

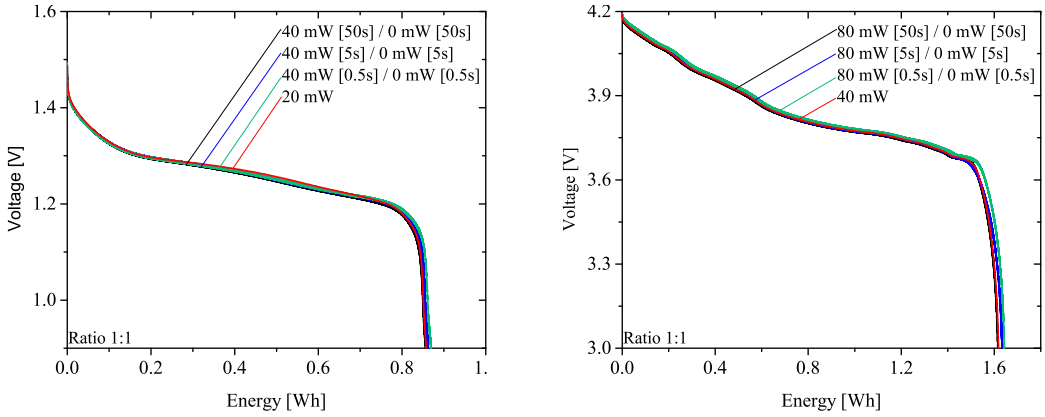

(a) NiMH (b) Li-Ion

Fig. 12: Continuous and intermittent discharge of NiMH and Li-Ion cells with $(T_{\mathrm{ON}}/T_{\mathrm{OFF}})$ ratio of 1:1. Discharge powers are indicated along with T_{ON} and T_{OFF} times in square brackets.

no potential charge recovery effect was observed within the operating power range of WSNs.

6. ELECTROCHEMICAL EFFECTS IN BATTERY CELLS

In this section, we elucidate the underlying electrochemical phenomena of batteries, which are mainly responsible for our results obtained in Section 5.3. Moreover, we provide clear reasoning of why a charge recovery cannot take place in real battery cells as claimed in the literature. In addition, the fundamental operations of an electrochemical cell along with a focus on overpotential and rate capacity effect are explained.

6.1. Electrochemical Cell

Batteries are electrochemical storage devices, which implies a chemical reaction coupled with an electron transfer. The schematic in Fig. 13 gives an overview of the basic components inside a battery. During discharge, shuttle ions (M^+) are oxidized at the anode (Eq. (6)) and release electrons (e^-), which travel through the outer circuit to power the load. Oxidized shuttle ions inside the battery move through the electrolyte to the cathode side, where they are reduced by electrons coming through the load (Eq. (7)). This happens spontaneously because the cathode material is chosen such that it forms a chemically favorable (very negative Gibbs free energy) reaction product with the metal anions. The separator prevents flow of electrons through the electrolyte, forcing them through the outer circuit in order to power the load.

$$Anode\colon M \rightarrow M^+ + e^- \qquad (Oxidation) \tag{6}$$

$$Cathode\colon M^+ + e^- \rightarrow M \qquad (Reduction) \tag{7}$$

Self-replenishment of active materials. While other effects such as temperature changes might have an impact in the energy output obtained from the battery, the *so-called* recovery effect is often explained as self-replenishment of the active materials during an intermittent discharge by most of the existing works referenced in Section 2. From an electrochemical point of view, this means, that the oxidized shuttle ion (M^+) would travel back to the active side of the anode and be reduced again by an electron from the external circuit. Whereas, during an intermittent discharge, no electrons are supplied from the outer circuit and hence no real charge recovery is pos-

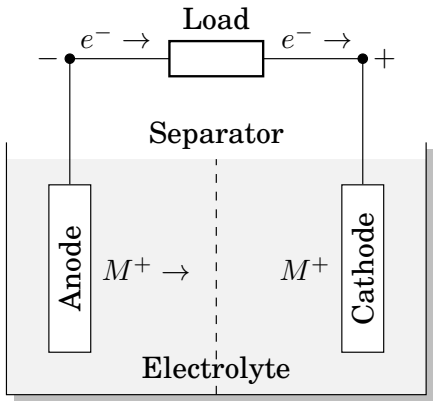

Fig. 13: Battery schematic during discharge. Shuttle ions (M^+) are oxidized at the anode and move towards the cathode inside the cell. The electron (e^-) released during oxidation travel through the outer circuit to power the load.

sible. Therefore, the edges ($P_j(k)$) corresponding to charge recovery in the stochastic battery models shown in Fig. 3 are invalid from an electrochemical perspective since no self-replenishment of active materials takes place in the cell.

6.2. Overpotential and Rate Capacity Effect

In this section, we explain the overpotential of a battery, which is the fundamental principle of the electrochemical phenomenon called rate capacity effect. The reduced energy output or runtime of an intermittent discharge compared to a continuous discharge observed in our experimental results in Section 5.3 is explained based on the overpotential and rate capacity effect.

Overpotential. In the context of this paper, the overpotential describes the fact that whenever a current is drawn from a battery, the voltage of that battery will drop depending upon the magnitude of the current drawn. The equilibrium voltage of the cell is defined as the cell voltage at chemical equilibrium of the battery at a given SoC and temperature; it can be expressed as E_0. In theory, to obtain maximum energy output from a battery, the cell voltage E_T should follow the discharge profile of the equilibrium voltage E_0. However, the cell voltage deviates from the equilibrium voltage as soon as a current is drawn from the cell. This deviation is termed as overpotential η and can be expressed as:

$$\eta = E_0 - E_\mathrm{T} \tag{8}$$

The overpotential is caused by various kinetic limitations and can be divided into three main parts: ohmic overpotential (η_ohmic), activation overpotential ($\eta_\mathrm{activation}$) and concentration overpotential ($\eta_\mathrm{concentration}$) [Winter and Brodd 2004]:

$$\eta = \eta_\mathrm{ohmic} + \eta_\mathrm{activation} + \eta_\mathrm{concentration} \tag{9}$$

The ohmic overpotential is governed by Ohm's law and arises from internal resistances of the ion conducting electrolyte and the electron conducting construction materials of the battery (electrodes, current collector, terminals). The activation overpotential, also known as electron transfer overpotential, arises from kinetic hindrance during the charge-transfer reaction and can be described by the ButlerVolmer and Tafel equations [Bard and Faulkner 1980]. The concentration overpotential is caused by limited mass transport when diffusion arises from a gradient in concentration and can be described by Fick's laws. The practical relevance of the overpotentials is best understood in a scenario where a constant current I_ext flows through a load. The same current is then flowing through every interface and along every path in the battery cell. If the

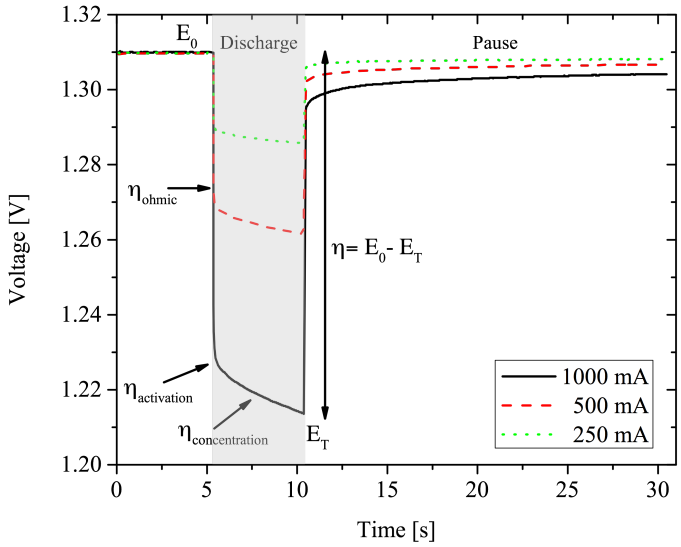

Fig. 14: Measured influence of the power rate on the overpotential and the voltage relaxation of a NiMH cell.

transport of shuttle ions (M^+) or electrons (e^-) is hindered at a position X along this path, the enforced external current I_{ext} builds up a local polarization and thus an electric field. This field adds additional driving force to the ions (or electrons) at position X. The field becomes stronger until it is just sufficient to locally create a current I_{local} at position X that is equal to the external current I_{ext}. The local polarization voltage (overpotential), associated with this field, however, diminishes the externally available voltage E_{T} as compared to the theoretical cell voltage E_0. A detailed review of different sources of overpotentials and their underlying mechanism is explained in [Park et al. 2010], [Bernardi and Go 2011].

The total overpotential is a function of current rate, SoC, temperature, battery chemistry, battery design and age of the battery. The influence of power rate on the overpotential is crucial to understand the experimental results in Section 5.3. Fig. 14 illustrates the measured effect of different power rates on the overpotential and the voltage relaxation behavior of a NiMH battery. The cell was given a $5\,$s pulse (discharge) with currents of 250, 500 and $1000\,$mA and allowed to rest after (pause). It was found that the higher the power rate, the higher the overpotentials. The influence of power rate on each individual overpotential (η_{ohmic}, $\eta_{\text{activation}}$, $\eta_{\text{concentration}}$) depends on many factors, however, all overpotentials will increase with increasing power rate. Intermittent discharge always has a higher peak power and therefore a higher overpotential compared to the continuous discharge with the equivalent average power.

The different overpotentials have different time responses as shown in Fig. 14 depending on the underlying processes. The ohmic overpotential is very fast and appears instantaneously (microseconds), the activation overpotential occurs in the range of milliseconds and the concentration overpotential is in the range of seconds up to hours [Jossen 2006]. The different time responses of the overpotential have an influence on the energy output obtained from the battery and therefore they are required to be considered while optimizing the communication data traffic of the WSN as explained in Section 7.2.

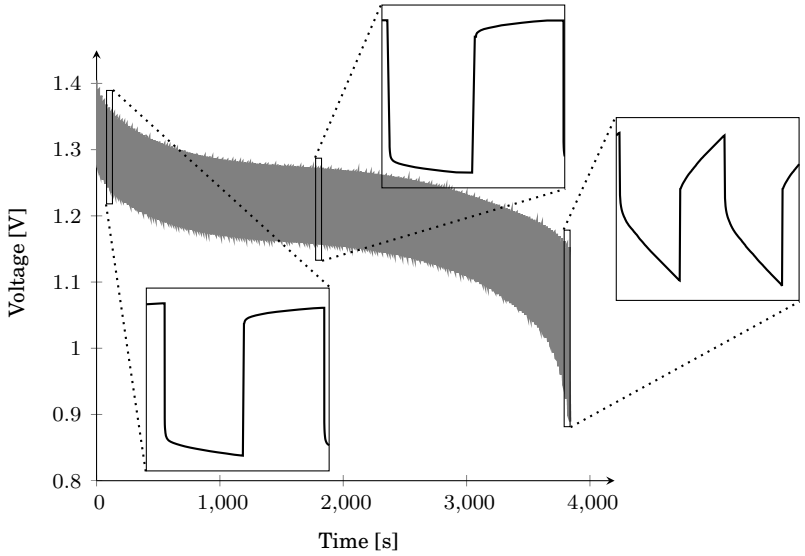

Fig. 15: Measured influence of different overpotentials during an intermittent discharge of a NiMH cell. As seen from the graph, the ohmic overpotential is dominating at higher SoC values and the concentration overpotential is more prominent towards the end of discharge

Rate capacity effect. In battery terminology, the C-rate is often used to define the charge or discharge current of a battery. 1C corresponds to the current necessary to charge or discharge the battery completely in one hour. A 2C rate would be the equivalent current to charge or discharge a battery in half an hour and 0.5C corresponds to two hours of charge or discharge. This definition makes it easier to compare batteries with different capacities and quickly access their power capabilities. The rate capacity effect descibes the decrease of usable capacity of a battery with increasing C-rates. The relation between the discharge current and the battery output capacity is modeled by Peukert's law as

$$I_{\text{batt}}^{n} \cdot t = C \tag{10}$$

where t is the time required to discharge the battery at current I_{batt}, C is the capacity of the battery in A h and n is the Peukert constant. The Peukert constant depends upon the type of battery and it is directly related to the internal resistance of the cell [Rekioua 2014]. Typically, the different overpotentials (η_{ohmic}, $\eta_{\text{activation}}$ and $\eta_{\text{concentration}}$), reflect the resistance of the cell and this is the reason for batteries to show a rate capacity effect. As explained previously, the overpotentials are a complex function of several terms such as temperature, current rate, SoC, battery chemistry, cell design (high power or high energy cell), age of the battery, etc. [Pop et al. 2008]. Therefore, it is difficult to model the individual contribution of different overpotentials to the rate capacity effect. A rough estimation regarding the contribution of different overpotentials is possible from Fig. 14, where we observe that the ohmic overpotential (η_{ohmic}) is dominating the other overpotentials ($\eta_{\text{activation}}$ and $\eta_{\text{concentration}}$) in this specific SoC value.

Nevertheless, to further understand the influence of different overpotentials on the rate capacity effect, we performed an intermittent discharge experiment with a NiMH cell. The test pattern consists of $10\,\text{s}$ T_{ON} time with $1000\,\text{mA}$ discharge current followed by $10\,\text{s}$ of rest with $0\,\text{mA}$. The experiment was repeated till the cell voltage reached its cut-off value of $0.9\,\text{V}$ as specified in its datasheet. Magnifications of the voltage profile at three different SoC values (fully charged, partially discharged and towards end of

discharge) are provided. It can be seen that, at high SoC values, the drop due to the ohmic overpotential is higher compared to other overpotentials. Even though we can observe some contribution from the activation overpotential at this SoC range, it is not significant compared to the drop due to the ohmic overpotential. At the partially discharged state, the rate capacity effect of the cell is mainly dominated by the ohmic overpotential, as seen in Fig. 15. On the other hand, towards the end of discharge, the voltage drop due to the concentration overpotential becomes prominent. This is because the shuttle ions that are moving inside the cell from anode to cathode, as explained in Section 6.1, are limited with their mobility. This in turn obstructs the arrival of further shuttle ions towards the cathode and this obstruction results in a higher overpotential as shown in Fig. 15. To summarize, for this specific NiMH cell, at full and partially charged states, the ohmic overpotential dominates and towards the end of the discharge, the concentration overpotential becomes more significant. Nevertheless, the usable energy and the average voltage of the battery decrease with increasing power rates. Therefore, in order to obtain higher energy output and thereby a longer battery runtime, the discharge current rate of the battery has to be reduced in order to mitigate the rate capacity effect.

Summary. In summary, underlying electrochemical processes strongly depend on the cell chemistry, the design of the battery and external factors like current rate and temperature. From an electrochemical point of view, self-replenishment of active materials does not take place during the idle periods of an intermittent discharge. Therefore the intermittent discharge has no benefit compared to a continuous discharge performed with the equivalent average power.

7. MODEL AMENDMENTS AND POWER MANAGEMENT TECHNIQUES

Based on our experimental results obtained in Section 5.3 and the electrochemical explanation of battery behavior provided in Section 6, in this section we suggest necessary amendments for the stochastic battery models explained in Section 3.1. Moreover, we outline both hardware and software based power management techniques to increase the runtime of the WSN by reducing the rate capacity effect.

7.1. Recommended Amendments to Existing Stochastic Battery Models

From our experimental evaluations in Section 5, we identify that the intermittent discharge of the battery provided less energy output or runtime when compared with the corresponding continuous discharge performed with equivalent average power. This implies that the charge recovery does not occur in these battery chemistries during the idle periods of an intermittent discharge as claimed by the existing literature. Moreover, as explained in Section 6, from an electrochemical perspective it is not possible for a battery to recover charge during the idle periods of an intermittent discharge as claimed in the literature. The self replenishment of active materials inside the battery does not happen spontaneously because the battery cell requires an electron from the outer circuit to reduce the oxidized shuttle ions at the anode side. Since the external circuit, if it is not a charging device, does not supply electrons, this reaction is infeasible in case of a real battery cell. Therefore, we suggest that the charge recovery edges ($P_j(k)$) in the existing Markov chain model shown in Fig. 3 should be removed, since the self-replenishment of active materials does not take place during an intermittent discharge. With these changes, the stochastic model with recovery effect gets transformed into a battery discharge model.

7.2. Power Management Techniques

In this section, we suggest hardware and software based approaches for power management that can be used to improve the energy output obtained from the battery by reducing the rate capacity effect.

Hardware based power management approaches. Discharging the battery with high peak power decreases the overall energy output, because of the rate capacity effect. This is observed from our experimental results shown in Table II, where the

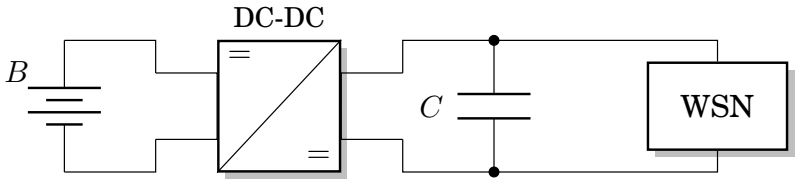

Fig. 16: Hybrid power supply architecture for obtaining higher energy output from the battery by minimizing the rate capacity effect [Shin et al. 2011]. The supercapacitor C handles the higher peak power experienced during an intermittent discharge and is efficiently charged at a lower continuous discharge rate from the battery B using the DC-DC converter.

continuous discharge test with $8\,\text{mW}$ discharge power provided an energy output of $1.6\,\text{W h}$ and the corresponding intermittent discharge test with $(T_{\text{ON}}/T_{\text{OFF}})$ ratio of 1:4 ($40\,\text{mW}[50\,\text{s}]$ / $0\,\text{mW}[200\,\text{s}]$) provided an energy output of $1.48\,\text{W h}$. An energy gain of approximately 8% was obtained for this continuous discharge test compared to the corresponding intermittent discharge test. This is equivalent of comparing the power supply configuration A (cells are connected in parallel) to the power supply configuration B (cells are switched periodically) as shown in Fig. 6 for $N = 5$. Therefore, from these experiments, it can be concluded that configuration A performs better than configuration B because of the reduced peak power drawn from the cell. This observation is a clear contradiction to the results obtained based on stochastic battery models in [Chiasserini and Rao 2001a] where it is claimed that switching between multiple batteries to power the WSN yields longer runtime than the constant parallel-connected battery setup due to the charge recovery effect. By contrast, our experimental results show that switching between the batteries provides reduced energy output compared to operating them in parallel. This applies to all tests performed on alkaline cells according to the evaluation procedure in Table I. Therefore, instead of switching between the batteries in a multiple-battery power supply architecture, we suggest to operate them in a constant-parallel connected fashion (configuration A) in order to obtain a higher energy output by reducing the peak power drawn from each cell.

In certain applications a multiple-battery setup is not possible due to size and weight constraints. In such cases, the existing power management approaches turn OFF the WSN during inactive periods in order to reduce the power drawn from the battery. However, for a battery this behaves like an intermittent discharge with ON periods followed by OFF periods and as shown from our experimental results that a continuous discharge with equivalent average power provides higher energy output than performing an intermittent discharge. Therefore, in such cases we recommend a battery-supercapacitor hybrid power supply architecture as shown in Fig. 16, where a supercapacitor is accompanied with a battery to mitigate the rate capacity effect due to the intermittent discharge as proposed in [Shin et al. 2011]. Having the advantage of high power density compared to that of batteries, supercapacitors efficiently handle higher peak powers as experienced during an intermittent discharge. Higher energy output or runtime is obtained by charging the supercapacitor at a reduced average power from the battery and optimally scheduling the wake-up/sleep time of the WSN considering the amount of charge present in the supercapacitor ([Tanevski et al. 2013]).

Software based power management approaches. Apart from the hardware based power management solutions, the energy output of the battery might be maximized through appropriate scheduling of the communication data. From Table II and Figure 9a, we can see that for the same $(T_{\text{ON}}/T_{\text{OFF}})$ ratio of 1:1, the test case with a shorter T_{ON} and T_{OFF} time ($40\,\text{mW}[0.5\,\text{s}]/0\,\text{mW}[0.5\,\text{s}]$) provided an energy output of $1.49\,\text{W h}$. However, the test cases $40\,\text{mW}[5\,\text{s}]/0\,\text{mW}[5\,\text{s}]$ and $40\,\text{mW}[50\,\text{s}]/0\,\text{mW}[50\,\text{s}]$, even though with a longer rest period compared to the former test case, resulted in a reduced energy output of $1.44\,\text{W h}$ and $1.43\,\text{W h}$, respectively. As discussed in Sec-

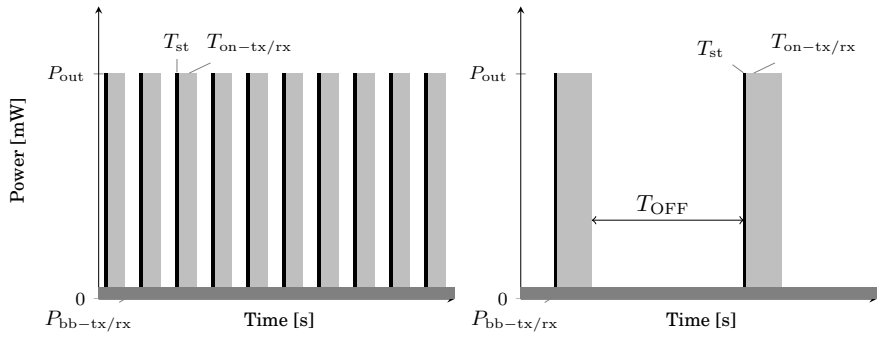

(a) Shorter T_{ON} and T_{OFF} (b) T_{OFF} longer than T_{ON}

Fig. 17: Scheduling the wake-up/sleep time of the WSN to obtain higher energy output considering the electrochemical properties of the battery. (a) A shorter T_{ON} and T_{OFF} is more favorable and (b) on the other hand if shorter T_{ON} time is not possible then a longer T_{OFF} time is required to compensate the concentration overpotential.

tion 6, the concentration overpotential is visible only in the time domain of seconds and due to the shorter T_{ON} time of $0.5\,\text{s}$, the battery has a reduced overall overpotential, especially at the end of discharge. On the other hand, the test cases with T_{ON} times of $5\,\text{s}$ and $50\,\text{s}$ have a higher overall overpotential and therefore the energy output of these tests is lower, even though their T_{OFF} times are larger than the test case $40\,\text{mW}[0.5\,\text{s}]/0\,\text{mW}[0.5\,\text{s}]$. This indicates that a periodic data transfer mode, as explained in Fig. 7a, with shorter T_{ON} time does not enter the time domain of the concentration overpotential of the battery. On the other hand, buffering the data for a longer time and transmitting in a burst mode as shown in Fig. 7b results in a reduced energy output due to longer T_{ON} time. However, increasing the value of T_{OFF} allows the cell to relax and to compensate the concentration overpotential induced by the longer T_{ON} time (Fig. 9b and 9c). Therefore, we suggest that while optimizing the wake-up/sleep time of the WSN, the electrochemical properties of the battery such as overpotential and rate capacity effect should also be considered along with the start-up losses in the transceiver. A shorter T_{ON} and T_{OFF} time is more favorable and also saves cost in terms of buffer size required for holding incoming data during the T_{OFF} period. If shorter T_{ON} times are not possible to be scheduled in an application then the T_{OFF} value must be considerably larger than the T_{ON} value as shown in Fig. 17, in order to compensate for the higher concentration overpotential.

7.3. Future Work

Through our systematic experimental evaluations we identified that there is no existence of charge recovery effect in batteries. Moreover, we identify the rate capacity effect as the dominant electrochemical phenomenon that should be considered for maximizing the energy output of the battery power supply used in WSN applications. Our future work in this direction involves analyzing and characterizing the gain obtained from the hybrid power supply architecture consisting of batteries and supercapacitors outlined in the previous subsection. Moreover, developing optimal communication data shaping methodologies, considering the electrochemical properties discussed in this paper will be the focus of our future work.

8. CONCLUDING REMARKS

This paper provides an experimental evaluation of the battery recovery effect in the domain of WSNs. The general architecture of a typical WSN and two operating modes that have an impact on the energy output of the battery are analyzed in detail. In contrast to state-of-the-art approaches, which analyze the charge recovery effect in

batteries through stochastic battery models, this paper proposes a systematic evaluation procedure for experimentally verifying the existence of battery charge recovery effect. This evaluation procedure was used to verify three different battery chemistries (alkaline, NiMH and Li-Ion) using a high accuracy battery tester. The experimental results do not show any charge recovery effect by performing intermittent discharges on these three battery chemistries within the operating power range of WSNs. Moreover, the continuous discharge performed with equivalent average power of the intermittent discharge provided higher energy output due to the reduced peak power. Therefore, the dominant electrochemical phenomenon that governs the energy output of the battery is the rate capacity effect and no charge recovery takes place in these investigated battery chemistries. This analysis complies with the electrochemical explanation of the battery behavior during an intermittent discharge. Upon identifying that the rate capacity effect as the dominant electrochemical phenomenon, we outlined both hardware and software based power management approaches in order to obtain higher energy output from the battery by minimizing the rate capacity effect. As a part of future work, we will characterize the gain obtained from the hybrid power supply architecture consisting of a battery and a supercapacitor outlined in the previous subsection. Moreover, developing optimal communication data shaping methodologies, considering the electrochemical properties discussed in this paper will be the focus of our future work.

REFERENCES

I. F. Akyildiz, W. Su, Y. Sankarasubramaniam, and E. Cayirci. 2002. Wireless sensor networks: a survey. *Computer Networks*. 38, 4 (Jan 2002), 393 – 422. DOI:http://dx.doi.org/10.1016/S1389-1286(01)00302-4

G. Anastasi, M. Conti, and D. M. Francesco. 2009. Extending the Lifetime of Wireless Sensor Networks Through Adaptive Sleep. *IEEE Transactions on Industrial Informatics*. 5, 3 (Aug 2009), 351–365. DOI:http://dx.doi.org/10.1109/TII.2009.2025863

A. J. Bard and L. R. Faulkner. 1980. *Electrochemical methods: fundamentals and applications*. Wiley, New york, USA.

BaSyTec Tester 2013. Datasheet of BaSyTec CTS Battery Tester. (Mar 2013). http://www.basytec.de

L. Benini, D. Bruni, A. Macii, E. Macii, and M. Poncino. 2003. Discharge current steering for battery lifetime optimization. *IEEE Transactions on Computers* 52, 8 (Aug 2003), 985–995. DOI:http://dx.doi.org/10.1109/TC.2003.1223633

L. Benini, G. Castelli, A. Macii, E. Macii, M. Poncino, and R. Scarsi. 2001b. Extending Lifetime of Portable Systems by Battery Scheduling. In *Proceedings of the Conference on Design, Automation and Test in Europe*. IEEE, 197–203. DOI:http://dx.doi.org/10.1109/DATE.2001.915024

L. Benini, G. Castelli, A. Macii, and R. Scarsi. 2001a. Battery-driven dynamic power management. *IEEE Design and Test of Computers*. 18, 2 (Mar 2001), 53–60. DOI:http://dx.doi.org/10.1109/54.914621

D. M. Bernardi and J. Y. Go. 2011. Analysis of pulse and relaxation behavior in lithium-ion batteries. *Journal of Power Sources* 196, 1 (Jan 2011), 412–427. DOI:http://dx.doi.org/10.1016/j.jpowsour.2010.06.107

U. Boker, T. A. Henzinger, and A. Radhakrishna. 2014. Battery Transition Systems. *SIGPLAN Notices* 49, 1 (Jan 2014), 595–606. DOI:http://dx.doi.org/10.1145/2578855.2535875

S. Castillo, N. K. Samala, K. Manwaring, B. A. Izadi, and D. Radhakrishnan. 2004. Experimental Analysis of Batteries Under Continuous and Intermittent Operations. In *Proceedings of ESA/VLSI*. IEEE, 18–24.

C. K. Chau, F. Qin, S. Sayed, M. H. Wahab, and Y. Yang. 2010. Harnessing Battery Recovery Effect in Wireless Sensor Networks: Experiments and Analysis. *IEEE Journal on Selected Areas in Communication* 28, 7 (Sep 2010), 1222–1232. DOI:http://dx.doi.org/10.1109/JSAC.2010.100926

Y. Chenfu, W. Lili, and L. Ye. 2015. Energy Efficient Transmission Approach for WBAN Based on Threshold Distance. *IEEE Sensors Journal* 15, 9 (Sep 2015), 5133–5141. DOI:http://dx.doi.org/10.1109/JSEN.2015.2435814

C. F. Chiasserini and R. R. Rao. 1999a. A model for battery pulsed discharge with recovery effect. In *Proceeding of Wireless Communications and Networking Conference*. IEEE, 636 – 639. DOI:http://dx.doi.org/10.1109/WCNC.1999.796721

C. F. Chiasserini and R. R. Rao. 1999b. Pulsed Battery Discharge in Communication Devices. In *Proceedings of fifth Annual International Conference on Mobile Computing and Networking*. ACM, 88–95. DOI:http://dx.doi.org/10.1145/313451.313488

C. F. Chiasserini and R. R. Rao. 2001a. Energy efficient battery management. *IEEE Journal on Selected Areas in Communications* 19, 7 (Jul 2001), 1235–1245. DOI:http://dx.doi.org/10.1109/49.932692

C. F. Chiasserini and R. R. Rao. 2001b. Improving battery performance by using traffic shaping techniques. *IEEE Journal on Selected Areas in Communications* 19, 7 (Jul 2001), 1385–1394. DOI:http://dx.doi.org/10.1109/49.932705

J. Choi and H. Cha. 2010. A Processor Power Management Scheme for Handheld Systems Considering Off-Chip Contributions. *IEEE Transactions on Industrial Informatics* 6, 3 (Aug 2010), 255–264. DOI:http://dx.doi.org/10.1109/TII.2010.2050330

P. Chowdhury and C. Chakrabarti. 2005. Static task-scheduling algorithms for battery-powered DVS systems. *IEEE Transactions on Very Large Scale Integration (VLSI) Systems* 13, 2 (Feb 2005), 226–237. DOI:http://dx.doi.org/10.1109/TVLSI.2004.840771

S. Dasika, S. Vrudhula, K. Chopra, and R. Srinivasan. 2004. A Framework for Battery-Aware Sensor Management. In *Proceedings of the Conference on Design, Automation and Test in Europe*. 962–967. DOI:http://dx.doi.org/10.1109/DATE.2004.1269017

M. Day. 2009. Using power solutions to extend battery life in MSP430 applications. In *App note Texas Instruments*. http://www.ti.com/lit/an/slyt356/slyt356.pdf

M. Dhanaraj, S. Jayashree, and C. S. R. Murthy. 2005. A Novel Battery Aware MAC Protocol for Minimizing Energy X Latency in Wireless Sensor Networks. In *High Performance Computing*. Lecture Notes in Computer Science, Vol. 3769. Springer Berlin Heidelberg, 312–321. DOI:http://dx.doi.org/10.1007/11602569_34

R. W. Erickson and D. Maksimovic. 2001. *Fundamentals of power electronics, 2nd edition*. Springer.

T. F. Fuller, M. Doyle, and J. Newman. 1994. Relaxation Phenomena in Lithium-Ion-Insertion Cells. *Journal of The Electrochemical Society* 141 (Jan 1994), 982–990. DOI:http://dx.doi.org/10.1149/1.2054868

GSP Li-Ion 2012. Datasheet of GSP062530 Li-Polymer cell. (Jun 2012). http://www.greatpowerbattery.com.hk/rechargeable.html

M. Horton, D. Culler, K. Pister, J. Hill, R. Szewczyk, and A. Woo. 2002. MICA, The Commercialization of Microsensor Motes. *Sensors Magazine* 19 (Apr 2002), 40–48. http://www.sensorsmag.com/networking-communications/mica-the-commercialization-microsensor-motes-1070

S. Jayashree, B. S. Manoj, and C. S. R. Murthy. 2004. On Using Battery State for Medium Access Control in Ad Hoc Wireless Networks. In *Proceedings of the 10th Annual International Conference on Mobile Computing and Networking*. ACM, 360–373. DOI:http://dx.doi.org/10.1145/1023720.1023755

M. R. Jongerden and B. R. Haverkort. 2009. Which battery model to use? *IET Software* 3, 6 (Dec 2009), 445–457. DOI:http://dx.doi.org/10.1049/iet-sen.2009.0001

M. R. Jongerden, A. Mereacre, H. Bohnenkamp, B. R. Haverkort, and J. Katoen. 2010. Computing Optimal Schedules of Battery Usage in Embedded Systems. *IEEE Transactions on Industrial Informatics* 6, 3 (Aug 2010), 276–286. DOI:http://dx.doi.org/10.1109/TII.2010.2051813

A. Jossen. 2006. Fundamentals of battery dynamics. *Journal of Power Sources* 154, 2 (Mar 2006), 530–538. DOI:http://dx.doi.org/10.1016/j.jpowsour.2005.10.041

H. Junyoung, H. Jiman, and C. Yookun. 2009. EARQ: Energy Aware Routing for Real-Time and Reliable Communication in Wireless Industrial Sensor Networks. *IEEE Transactions on Industrial Informatics* 5, 1 (Feb 2009), 3–11. DOI:http://dx.doi.org/10.1109/TII.2008.2011052

R. M. LaFollette. 1995. Design and performance of high specific power, pulsed discharge, bipolar lead acid batteries. In *Proceedings of Tenth Annual International Battery Conference on Applications and Advances*. IEEE, 43–47. DOI:http://dx.doi.org/10.1109/BCAA.1995.398511

K. Lahiri, S. Dey, D. Panigrahi, and A. Raghunathan. 2002. Battery-Driven System Design: A New Frontier in Low Power Design. In *Proceedings of the Asia and South Pacific Design Automation Conference*. IEEE, 261–267. DOI:http://dx.doi.org/10.1109/ASPDAC.2002.994932

R. Min, M. Bhardwaj, S. Cho, E. Shih, A. Sinha, A. Wang, and A. Chandrakasan. 2001. Low-power wireless sensor networks. In *Proceedings of Fourteenth International Conference on VLSI Design*. 205–210. DOI:http://dx.doi.org/10.1109/ICVD.2001.902661

L. Mo, W. Yajun, and W. Yu. 2011. Complexity of Data Collection, Aggregation, and Selection for Wireless Sensor Networks. *IEEE Transactions on Computers* 60, 3 (Mar 2011), 386–399. DOI:http://dx.doi.org/10.1109/TC.2010.50

R. F. Nelson, R. Rinehart, and S. Varley. 1997. Ultrafast pulse discharge and recharge capabilities of thin-metal film battery technology. In *Proceddings of the 11th International Pulsed Power Conference (Digest of Technical Papers)*, Vol. 1. IEEE, 636–641. DOI:http://dx.doi.org/10.1109/PPC.1997.679411

P. Nuggehalli, V. Srinivasan, and R. R. Rao. 2006. Energy efficient transmission scheduling for delay constrained wireless networks. *IEEE Transactions on Wireless Communications* 5, 3 (Mar 2006), 531–539. DOI:http://dx.doi.org/10.1109/TWC.2006.1611083

Panasonic NiMH 2000. Datasheet of HHR-75AAA/HT NiMH cells. (May 2000). http://www.actec.dk/Panasonic/pdf/HHR75AAA.pdf

M. Park, X. Zhang, M. Chung, G. B. Less, and A. M. Sastry. 2010. A review of conduction phenomena in Li-ion batteries. *Journal of Power Sources* 195, 24 (Dec 2010), 7904–7929. DOI:http://dx.doi.org/10.1016/j.jpowsour.2010.06.060

F. D. Pellegrini, D. Miorandi, S. Vitturi, and A. Zanella. 2006. On the use of wireless networks at low level of factory automation systems. *IEEE Transactions on Industrial Informatics* 2, 2 (May 2006), 129–143. DOI:http://dx.doi.org/10.1109/TII.2006.872960

L. Peng, Q. Chunming, and W. Xin. 2004. Medium access control with a dynamic duty cycle for sensor networks. In *Proceedings of Wireless Communication and Networking Conference*, Vol. 3. IEEE, 1534–1539. DOI:http://dx.doi.org/10.1109/WCNC.2004.1311671

J. Polastre, J. Hill, and D. Culler. 2004. Versatile Low Power Media Access for Wireless Sensor Networks. In *Proceedings of the 2nd International Conference on Embedded Network Sensor Systems*. ACM, 95–107. DOI:http://dx.doi.org/10.1145/1031495.1031508

V. Pop, H. J. Bergveld, D. Danilov, P. P. L. Regtien, and P. H. L. Notten. 2008. *Battery management systems: accurate state-of-charge indication for battery powered applications* (springer verlag ed.). Vol. 9. Springer Verlag. DOI:http://dx.doi.org/10.1007/978-1-4020-6945-1

W. Qing, Q. Qinru, and M. Pedram. 2000. An interleaved dual-battery power supply for battery-operated electronics. In *Proceedings of the Asia and South Pacific Design Automation Conference*. IEEE, 387–390. DOI:http://dx.doi.org/10.1109/ASPDAC.2000.835130

V. Raghunathan, C. Schurgers, P. Sung, and M. B. Srivastava. 2002. Energy-aware wireless microsensor networks. *IEEE Signal Processing Magazine* 19, 2 (Mar 2002), 40–50. DOI:http://dx.doi.org/10.1109/79.985679

D. Rakhmatov and S. Vrudhula. 2003. Energy Management for Battery-powered Embedded Systems. *ACM Transactions on Embedded Computing Systems* 2, 3 (Aug 2003), 277–324. DOI:http://dx.doi.org/10.1145/860176.860179

R. Rao, S. Vrudhula, and N. Chang. 2005. Battery Optimization vs Energy Optimization: Which to Choose and when?. In *Proceedings of the International Conference on Computer-aided Design*. 439–445. DOI:http://dx.doi.org/10.1109/ICCAD.2005.1560108

Recovery Effect Results 2015. Recovery effect measurement results repository. (2015). https://bitbucket.org/recoveryeffect/experimental-results.git

D. Rekioua. 2014. *Wind Power Electric Systems: Modeling, Simulation and Control*. Springer London. DOI:http://dx.doi.org/10.1007/978-1-4471-6425-8

P. Rong and M. Pedram. 2006. Battery-aware power management based on Markovian decision processes. *IEEE Transactions on Computer-Aided Design of Integrated Circuits and Systems* 25, 7 (Jul 2006), 1337–1349. DOI:http://dx.doi.org/10.1109/ICCAD.2002.1167609

S. Sarkar and M. Adamou. 2003. A framework for optimal battery management for wireless nodes. *IEEE Journal on Selected Areas in Communications* 21, 2 (Feb 2003), 179–188. DOI:http://dx.doi.org/10.1109/JSAC.2002.807335

E. Shih, S. Cho, F. S. Lee, B. H. Calhoun, and A. Chandrakasan. 2004. Design Considerations for Energy-Efficient Radios in Wireless Microsensor Networks. *Journal of VLSI signal processing systems for signal, image and video technology* 37, 1 (May 2004), 77–94. DOI:http://dx.doi.org/10.1023/B:VLSI.0000017004.57230.91

D. Shin, Y. Kim, J. Seo, N. Chang, Y. Wang, and M. Pedram. 2011. Battery-supercapacitor hybrid system for high-rate pulsed load applications. In *Proceedings of the Conference on Design, Automation and Test in Europe*. 1–4. DOI:http://dx.doi.org/10.1109/DATE.2011.5763295

A. Sinha and A. Chandrakasan. 2001. Dynamic power management in wireless sensor networks. *IEEE Design and Test of Computers* 18, 2 (Mar 2001), 62–74. DOI:http://dx.doi.org/10.1109/54.914626

M. Tanevski, A. Boegli, and P. Farine. 2013. Power supply energy optimization for ultra low-power wireless sensor nodes. In *IEEE Symposium on Sensors Applications*. 176–181. DOI:http://dx.doi.org/10.1109/SAS.2013.6493581

Varta Alkaline 2003. Datasheet of AAA-LR03 Alkaline cells. (Jul 2003). http://www.elektronik.ropla.eu/pdf/stock/vmb/lr03-aaa.pdf

A. G. Werner, K. Lorincz, M. Ruiz, O. Marcillo, J. Johnson, J. Lees, and M. Welsh. 2006. Deploying a wireless sensor network on an active volcano. *IEEE Journal on Internet Computing* 10, 2 (Mar 2006), 18–25. DOI:http://dx.doi.org/10.1109/MIC.2006.26

M. Winter and R. Brodd. 2004. What are batteries, fuel cells, and supercapacitors? *Chemical reviews* 104 (Sep 2004), 4245–4269. DOI:http://dx.doi.org/10.1021/cr020730k

W. Ye, J. Heidemann, and D. Estrin. 2004. Medium Access Control with Coordinated Adaptive Sleeping for Wireless Sensor Networks. *IEEE/ACM Transactions on Networking* 12, 3 (Jun 2004). DOI:http://dx.doi.org/10.1109/TNET.2004.828953

Received July 2015; revised December 2015; accepted February 2016